

## SWAT PARAMETERIZATION FOR IDENTIFICATION OF CRITICAL EROSION WATERSHEDS IN THE PIRAPAMA RIVER BASIN, BRAZIL

Jussara Freire de Souza Viana<sup>1\*</sup>, Suzana Maria Gico Lima Montenegro<sup>1</sup>,  
Bernardo Barbosa da Silva<sup>2</sup>, Richarde Marques da Silva<sup>3</sup>, and Raghavan Srinivasan<sup>4</sup>

<sup>1</sup>Department of Civil Engineering, Federal University of Pernambuco, Recife, Pernambuco, Brazil

<sup>2</sup>Department of Meteorology, Federal University of Campina Grande, Campina Grande, Paraíba, Brazil

<sup>3</sup>Department of Geosciences, Federal University of Paraíba, João Pessoa, Paraíba, Brazil

<sup>4</sup>Ecosystem Sciences and Management and Biological and Agricultural Engineering Departments, Texas A&M University, College Station, Texas, United States.

Received 7 November 2018; received in revised form 16 February 2019; accepted 8 March 2019

### Abstract:

The aim of this research is to estimate the sediment yield in the Pirapama River Basin and in the area of contribution of the Pirapama Reservoir and to identify areas susceptible to soil erosion for identification of critical erosion watersheds during the period from 2000 to 2010. This study was conducted to design a framework for evaluating and identifying critical erosion in Pirapama watershed, based on the tolerable erosion concept, by using the Soil and Water Assessment Tool (SWAT) model. SWAT was calibrated and validated for two streamflow stations (Cachoeira Tapada and Destilaria Inexport) for the period from 2000 to 2010. The results show that the simulated data for Cachoeira Tapada station were considered good (NS = 0.68 and  $R^2 = 0.71$ ) and very good (PBIAS = 1.46%). Regarding the statistical data in the validation, the values of NS (0.67),  $R^2$  (0.85), and PBIAS (19.18%) were considered good, very good, and satisfactory, respectively. The statistical data obtained in the calibration of the model for the fluvimetric station Destilaria Inexport indicated that the simulated data are considered very good, with  $R^2 = 0.84$ , NS = 0.81, and PBIAS = 2.33%. In the validation, the statistics showed values consistent with the literature, with NS = 0.72,  $R^2 = 0.86$ , and PBIAS = -19.11%, which are considered good, very good, and satisfactory, respectively. The estimated average sediment yield in the Pirapama River basin ranged from 0.10 to 129.90 ton/ha.yr. The results of the sediment yield estimates in the contribution area of the Pirapama Reservoir showed that the mean sediment yield of the sub-basins upstream of the Pirapama Reservoir was 61.49 ton/ha.yr for the period analyzed. According to the annual estimates performed, 5.59 ton/ha.yr of this amount reaches the Pirapama Reservoir, which corresponds to 9% of the soil losses incident in the area. Thus, the sub-basins upstream of the Pirapama Reservoir were identified as portions of the basin that are susceptible to the erosion process. Sediment yield in these portions can interfere with the volume of water of the Pirapama Reservoir when the eroded material is carried to the depth of the lake.

**Keywords:** Reservoir, Sediment yield, SWAT model.

© 2019 Journal of Urban and Environmental Engineering (JUEE). All rights reserved.

\* Correspondence to: Jussara Freire de Souza Viana, Tel.: +55 81 91470836. E-mail: jussarafsouza@yahoo.com.br

## INTRODUCTION

Accelerated sediment yield is considered a serious environmental threat to sustainable development all over the world. The presence of sediments in watercourses is a consequence of the erosion processes occurring in their drainage basins due to the expansion of agricultural activities. Erosion is a natural process characterized by the selective loss of soil materials, where surface layer materials are washed away by the action of water or wind. Soil erosion and consequent sediment transport in watercourses are dependent on many factors such as precipitation, surface runoff, cover, land use, topography, drainage network, and sediment characteristics. The transport of sediments through the channel is the final product of a series of processes, which start with the precipitation that falls on the basin, and along its path through the slopes, interacts with a set of variables such as vegetation cover, type of soil and rock, and type of use and anthropic occupation. The sediment transport and deposition process has several implications such as the loading of aggregate or non-particle pollutants, loss of quality of water intended for human consumption, imbalance of ecosystems due to turbidity, silting of reservoirs, and changes in river channel geometry (Ghafari *et al.*, 2017). Sediments also reduce water storage capacity, increase the maintenance cost of dams, and shorten the life of reservoirs.

Around the world, about 75 billion Mg of soil are eroded from lands (Pimentel *et al.*, 1995) and approximately 0.3% of the value of agricultural production is lost due to erosion each year (Den Biggelaar *et al.*, 2003), which directly affects rural livelihoods (Panagopoulos *et al.*, 2011) and challenges the achievement of the goal of food security (Corrado *et al.*, 2019). It is estimated that around two-thirds of the soil eroded is deposited in lakes and rivers (Pimentel, 1997). Although sediment yield is a natural phenomenon (related to the processes of weathering and erosion), anthropic interference in the environment potentiates its production, as in the case of dams, urban development, channelization, and channel rectification (Kirkby, 1990). A high concentration of sediment in rivers can compromise or restrict water use. Projects involving dams, abstractions, and water treatment plants, for example, are directly influenced by the presence of sediments in the water source, as are the aquatic organisms and those that consume the water in its raw state directly from the river (Santos *et al.*, 2015).

Runoff-erosion models are useful tools to help understand the processes that occur in a watershed as well as to more realistically predict the transformation of precipitation into surface runoff and sediment yield and other elements of the hydrological cycle. The Soil and Water Assessment Tool (SWAT) model has been

used in several parts of the world to simulate different physical processes in a watershed and by integration of the model with Geographic Information Systems (GIS), which makes the process of manipulating the input and output data easier. This model was developed with the purpose of estimating the impact of different agricultural practices on water quantity and quality, soil loss, and pollutant load in watersheds (Neitsch *et al.*, 2011). The use of this type of model allows prediction of environmental impacts and optimization of management costs.

Erosion studies of this type are extremely important for the Northeast Region of Brazil, which is greatly affected by soil erosion due to high rainfall variability and increasing changes in soil use and occupation. As yet, there are few studies on erosion in this region, mainly in basins of the coastal portion of Northeast Brazil, as is the case of the Pirapama River basin.

Since 2001, the Pirapama River basin has been one of the main sources of water supply in the Metropolitan Region of Recife (MRR). However, at present, the basin is suffering serious problems in relation to environmental degradation of its water courses due to continuous deforestation of the natural vegetation, occupation of the territory by dwellings, and the development of agroindustrial activities, characterized by extensive areas of sugarcane cultivation. Therefore, it is understood that, due to such factors, studies to evaluate erosion in the basin and identify the areas most susceptible to such process are urgent, since through carrying out this type of study it is possible to apply mitigation measures that minimize the impacts arising from environmental problems in the basin, caused mostly by anthropogenic actions.

Therefore, this study aims to estimate sediment yield in the Pirapama River basin and in the area of contribution of the Pirapama Reservoir and to identify areas susceptible to soil erosion through the SWAT model for the period from 2000 to 2010.

## MATERIALS AND METHODS

### Study Area

The study was developed in the Pirapama River Basin, situated in the central portion of the MRR and in the Zona da Mata Pernambucana, more precisely between latitudes 8° 07' 29" and 8° 21' 00" S and longitudes 34° 56' 20" and 35° 23' 13" W. The basin has an area of approximately 600 km<sup>2</sup> with an extension of 80 km. Its source is in the city of Pombos, in the Agreste of Pernambuco, at an altitude of 450 m. Its outlet is located in the Jaboatão River, between the city of Cabo de Santo Agostinho and Jaboatão dos Guararapes (CPRH, 1998) (**Fig. 1**). The basin is bordered to the north by the

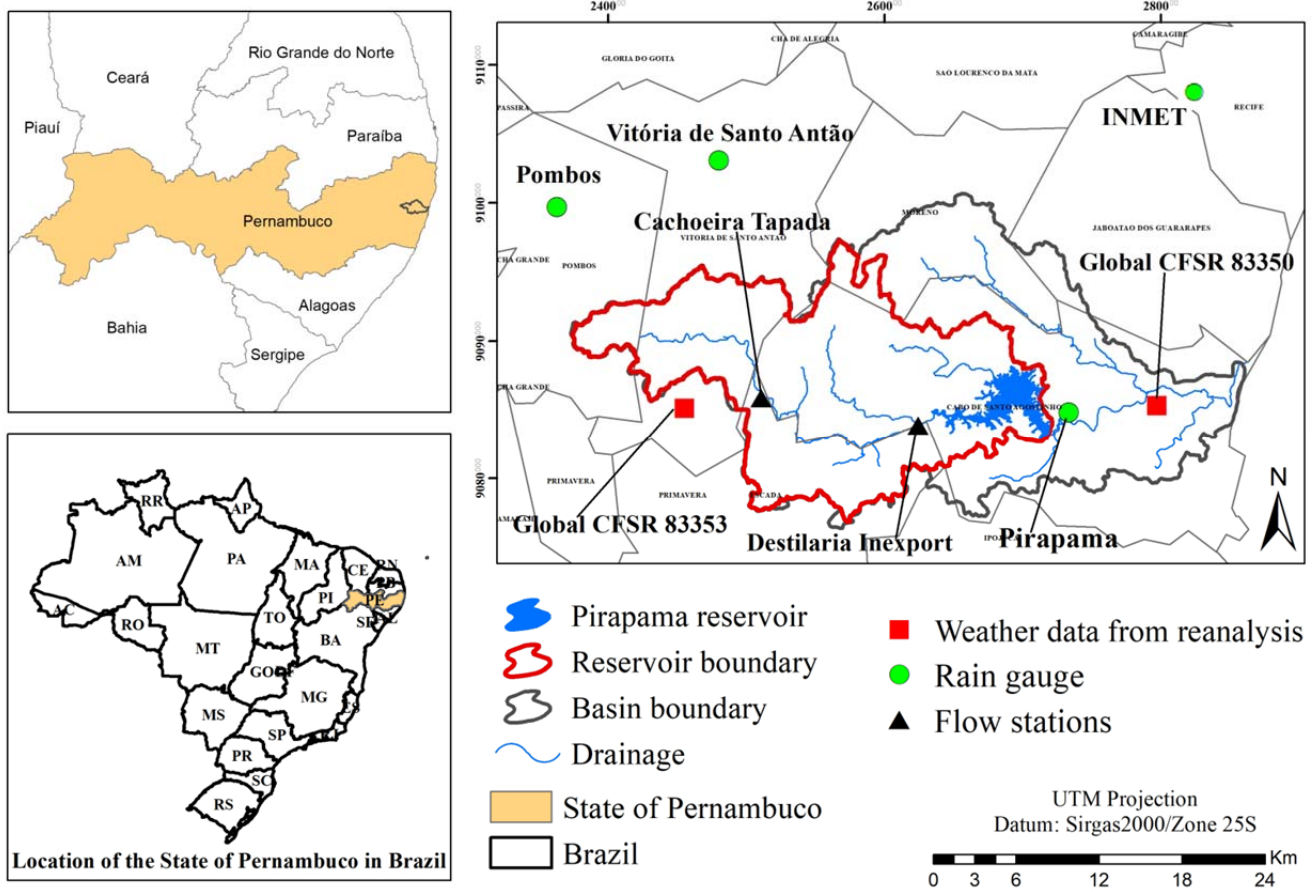


Fig. 1 Location of the Pirapama River basin and the stations used in the hydrological modelling of the basin – Pernambuco, Brazil.

basins of the Jaboatão and Tapacurá (tributary of Capibaribe) rivers, to the south and west by the Ipojuca River basin, and to the east by the Atlantic Ocean. There are two large flood-proofing reservoirs (Pirapama and Gurjaú reservoirs).

The Pirapama basin covers the area of seven cities: Cabo de Santo Agostinho, Jaboatão dos Guararapes, Ipojuca, and Moreno, which are located in the MRR, and Vitória de Santo Antão, Escada, and Pombos, in the Pernambucan Forest Zone. The largest proportion of the basin area is located in the city of Cabo de Santo Agostinho (57.2%), followed by Moreno (13.7%), Escada (11.8%), Vitória de Santo Antão (9.5%), Pombos (4.3%), and Jaboatão dos Guararapes (2.4%) (Fig. 1). The city of Ipojuca occupies only 1.1% of the area of the basin (Medeiros Braga *et al.*, 2013). Together, the cities that make up the basin have about 1,158,595 inhabitants, of which 84.4% live in urban areas (IBGE, 2010).

The use and occupation of the land of the Pirapama River basin is quite diverse, characterized by urban and industrial settings, small farms, polyculture (rural settlements), two small hydroelectric power stations, sugarcane cultivation areas, Atlantic forest, and mangroves (Santos & Silva, 2007).

The climate of the region is type As' (pseudo-tropical), warm and humid, according to Köppen's

climatic classification, with improvement of the strong solar radiation by trade winds. The monthly average temperature varies between 26 and 28 °C, while the relative air humidity is higher than 70% from March to September (CPRH, 2003). As for the rainfall regime, the region has two well-defined periods: dry, between September and February, with average monthly rainfall of less than 60 mm and evaporation that exceeds precipitation; and the rainy season, between March and August, in which the hydrological balance is generally positive. The annual averages of precipitation and evaporation in the region are around 1500 mm and 1200 mm, respectively (Stretta, 2000).

The relief is typical of crystalline modelling and includes hills and rounded mounds with altitudes above 60 m (Medeiros Braga *et al.*, 2013). The basin relief geology description is based on the morphological characteristics of the main collector, subdivided into three stretches: the upper, middle, and lower courses.

With regard to the pedology of the Pirapama River basin, the predominant soils in the area are red-yellow ultisol, yellow ultisol, and gleysols. To a lesser extent, psamment (close to the coast), nitisols, yellow oxisol, and mangrove soils occur in the basin (EMBRAPA, 2013).

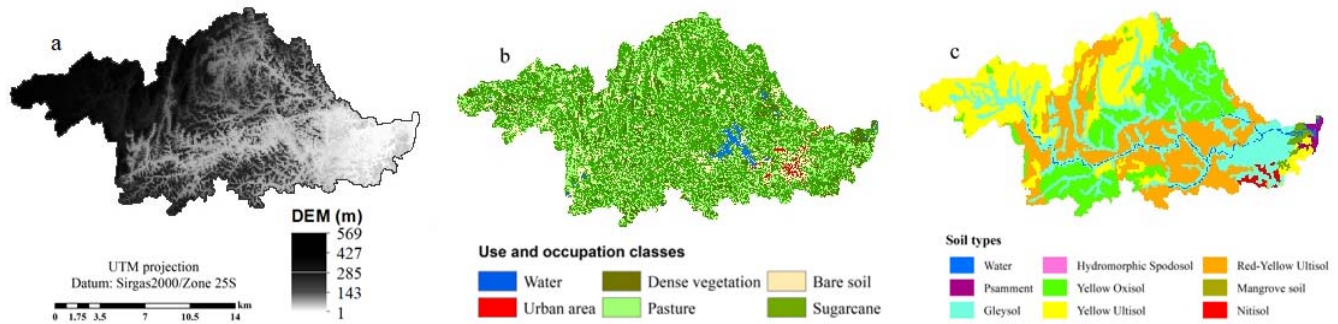


Fig. 2 Digital Elevation Model (a), land use (b), and soil types (c) of the Pirapama River basin.

Table 1. Association of SWAT land uses with present uses in the Pirapama River basin

Use and Occupation of Soil	SWAT Soil Uses	Area (Km <sup>2</sup> )	Area (%)
Water	Water (WATR)	7.37	1.23
Urban area	Urban (URBN)	4.82	0.80
Sugarcane	Sugarcane (SUGC)	313.54	52.27
Bare soil	Barren (BARR)	73.23	12.21
Dense vegetation	Forest – mixed (FRST)	63.72	10.62
Pasture	Pasture (PAST)	136.64	22.77

**Dataset**

In order to obtain the initial basin modelling, SWAT requires three different geospatial datasets: a digital elevation model (DEM), a map of soil types of the study area, and a land use map. The DEM used (Fig. 2a) has a spatial resolution of 30 m and was obtained from the website of the United States Geological Survey (USGS) at <http://earthexplorer.usgs.gov/>.

The land use and occupation map used in this study was based on two Landsat 5 satellite images with spatial resolution of 30 m (TM sensor, orbit 214, point 066) obtained from the National Institute of Space Research (INPE). The images are from 6 July 2005 and 28 July 2007 and were selected because they presented the least amount of clouds in the region. For the construction of the land use and occupation map, it was necessary to cut the two images and apply the image mosaic technique using the software ArcGIS 10.2, where a common point between the images was chosen to obtain the surrounding rectangle of the study area and make the land use map. In the process of classification of land use of the basin, the land use classes that were most evident in the region were defined using the supervised classification of the software ArcGIS 10.2, which determined six classes of land use, namely water, urban area, bare soil, dense vegetation, pasture, and sugarcane (Fig. 2b). After completing the classification process and the map composition, the existing land uses in the basin were associated with the land uses corresponding to the SWAT database after the introduction of this information plan in ArcSWAT. Table 1 shows the association of the land uses present in the basin with the uses in the SWAT model database.

The soil parameters followed the EMBRAPA Solos classifications obtained through the Internet portal for the Brazilian Soil Information System (<http://www.sisolos.cnptia.embrapa.br>) and some of the applied papers in Brazil, which defined values for some soil parameters (IBGE, 2007).

Soil information from the study area was entered directly into the model database. The soil type map was obtained from data provided by EMBRAPA Solos based on information provided by the Agroecological Zoning of Pernambuco (ZAPE), whose scale is 1:100.000 (Fig. 2c). This map was used as input data for basin modelling in SWAT in order to create Hydrological Response Units (HRUs). Table 2 shows the area occupied by each type of soil in the basin.

To estimate the discharge in the Pirapama River basin by the SWAT model, daily precipitation data were obtained from four rainfall stations in the field, and data from two weather stations and two flow stations were also used (Fig. 1). The daily data of the

Table 2. Area occupied by each type of soil present in the Pirapama River Basin

Types of Soil	Area (km <sup>2</sup> )	Area (%)
Gleysol	156.66	26.11
Hydromorphic spodosol	0.02	0.003
Mangrove soil	5.64	0.94
Nitisol	4.66	0.78
Psamment	4.18	0.70
Red-Yellow ultisol	157.09	26.18
Water	7.44	1.24
Yellow ultisol	145.79	24.30
Yellow oxisol	118.52	19.75

**Table 3.** Rainfall, streamflow, weather stations, and Tropical Rainfall Measuring Mission (TRMM) grid points used for this research

Code	Name	Type	Responsible	Latitude	Longitude
39195000	Destilaria Inexport	Flow	ANA	-8.16	-35.92
39192000	Cachoeira Tapada	Flow	ANA	-8.15	-35.15
83350	CFSR	Weather	NCEP	-8.27	-35.00
83353	CFSR	Weather	NCEP	-8.27	-35.31
82900	Recife-Curado	Rainfall	INMET	-8.05	-34.95
835138	Pirapama	Rainfall	ANA	-8.16	-35.03
835068	Vitória Sto. Antão	Rainfall	ANA	-8.64	-35.17
835137	Pombos	Rainfall	ANA	-8.08	-35.23

NCEP: National Centers for Environmental Prediction.

CFSR: Climate Forecast System Reanalysis.

climatological variables used for the modelling were obtained from two global grid points that are close to the basin, whose data are available through the Global Weather Data for SWAT website (<https://globalweather.tamu.edu>).

The flow and rainfall data were obtained from the National Water Agency (ANA), except for the Recife-Curado station, whose data were obtained from the National Institute of Meteorology (INMET). **Table 3** presents information about the rainfall, flow, and weather stations that were used in this research.

The flow rate stations used for this study were chosen because they presented observed flow data with a relevant period for the research. Thus, observed flow rate data were obtained for the 2000 to 2010 period, 2000–2006 for simulation and calibration and 2007–2010 for validation. The same periods as were used for calibration and validation were used to estimate the sediment yield.

For the selection of rainfall stations, those with data from the study period and with the lowest number of failures were considered (1997 to 2010). Thus, the 1997–2006 period was used for the initial simulation and calibration, with the years from 1997 to 1999 selected for model warm-up (adjusting the model to the natural conditions of the study area before presenting the results), and the period from 2007 to 2010 was used for validation, with a warm-up period from 2004 to 2006.

### Soil and Water Assessment Tool (SWAT) Model

The SWAT model was developed by the United States Department of Agriculture Agricultural Research Service (USDA-ARS). It can accomplish hydrological modelling of watersheds and analysis of many scenarios, such as the prediction of impacts of soil management on water quality, sediment transport, and transport of agricultural chemicals. It is a distributed physically based model, continuous in time, that simulates runoff, erosion in planes and channels, and transport of nutrients and pesticides on daily, monthly, and annual time scales (Aragão *et al.*, 2013; Neitsch *et*

*al.*, 2011). The hydrological model is based on the water balance equation, with a soil profile of 2 m depth as the control volume (Arnold *et al.*, 1998) (**Eq. 1**):

$$SW_t = SW_0 + \sum_{i=1}^t (R_d - Q_{sup} - E_a - W_{seep} - Q_{gw}) \quad (1)$$

where  $SW_t$  is the final soil water storage (mm),  $SW_0$  is the initial storage of water in soil on day  $i$  (mm),  $t$  is the time (days),  $R_d$  is the precipitation on day  $i$  (mm),  $Q_{sup}$  is the surface runoff on day  $i$  (mm),  $E_a$  is evapotranspiration on day  $i$  (mm),  $W_{seep}$  is percolation on day  $i$  (mm), and  $Q_{gw}$  is the return flow (capillary rise from the vadose zone) on day  $i$  (mm).

The surface runoff is estimated by two methods: the Soil Conservation Service (SCS) method and the Green Ampt infiltration method (Neitsch *et al.*, 2011). In this study, surface runoff was calculated using the Modified SCS Number Curve method.

$$Q_{sup} = \frac{(R_d - I_a)^2}{(R_d - I_a + S)} \quad (2)$$

in which  $Q_{sup}$  is the cumulative surface runoff or the excess precipitation (mm H<sub>2</sub>O),  $R_d$  is the precipitation level for the day (mm),  $I_a$  is the initial abstraction, which includes surface storage, interception, and initial infiltration (mm), and  $S$  is the retention parameter (mm).

The erosion and sediment yield in the SWAT model is calculated for the sub-basin and channels. The sediment yield from the runoff is computed for each sub-basin through the Universal Equation of Modified Soil Loss (MUSLE) (Williams, 1975). The SWAT sediment yield was calculated by Eq. 3:

$$Y = 11,8(Q_{sup} \cdot q_p \cdot A_{hru})^{0,56} \cdot K_{USLE} \cdot LS_{USLE} \cdot C_{USLE} \cdot P_{USLE} \cdot CFRG \quad (3)$$

in which  $Y$  is the sediment yield after day precipitation event (ton),  $Q_{sup}$  is the surface runoff (mm/ha),  $q_p$  is the peak flow rate (m<sup>3</sup>/s),  $A_{hru}$  is the area of the HRU in which the sediment input is estimated (ha),  $K_{USLE}$  is the soil erodibility factor (t h MJ<sup>-1</sup> mm<sup>-1</sup>),  $C_{USLE}$  is the land use and management factor,  $P_{USLE}$  is the factor



representing conservation practices,  $LS_{USLE}$  is the topographical factor, and CFRG is the roughness factor.

According to Neitsch *et al.* (2011), sediment transport in the drainage network occurs because of simultaneous processes of particle disintegration and deposition in the channel and its value is calculated using the simplified equation suggested by Bagnold (Williams, 1975).

After the estimation, the sediment yield information generated in SED\_OUT for each sub-basin was used, with its values being converted from tons to tons per hectare, taking as reference the area, in hectares, of the sub-basins. From the treatment and analysis of these data, the spatial distribution of sediment yield of the basin was applied using GIS techniques. In parallel, the spatial distribution of surface runoff and rainfall was also applied using GIS techniques, with the previous data treatment. To represent the spatial distribution of the rain, interpolation of the data was carried out using the Inverse Distance Weighting (IDW) method.

After that, estimates of the total sediment yield until the end outlet of the basin (SED\_OUT) were obtained. In this case, the area where the Pirapama Dam is located was defined as the end outlet of the basin (control point), because of the importance of the dam for the water supply of the RMR. Thus, the analysis of the total sediment yield was carried out only in the area of contribution of the Pirapama dam, taking into account the annual estimates (2000 to 2010).

In the SWAT modelling, the river basin is divided into sub-basins, whose number depends on the minimum drainage area. With the finalized delimitation, the model makes combinations of land uses, soil types, and slopes, which originate the HRUs. This research used ArcSWAT (version 2012.10.2.18), whose interface integrates the SWAT model in the GIS environment.

First, elevation data were automatically extracted for the drainage network and watershed using a DEM (Fig. 2a), and the watershed was divided into 29 sub-basins based on a drainage area threshold. By imputing reclassified land use data and reclassified soil data (Fig. 2b, c), the watershed was further divided into 1641 HRUs consisting of unique combinations of soil, land use/cover, and slope. Five categories of slope were defined for the HRUs: 0–3%, 3–8%, 8–20%, 20–45%, and > 45%. The HRU definition adopted multiple HRU methods. The percentage defined for the multiple HRUs was 0% for the three categories (land use and land cover classes, soil types, and slope). After these processes, meteorological and precipitation data were introduced into the model.

### Sensitivity analysis

The calibration and validation of the SWAT model was

preceded by the parameter sensitivity analysis, which analyses the influence of each parameter on the hydrological modelling process of the basin. For this research, 19 SWAT parameters that have the most influence on the flow in the model were selected based on the recommendations of Arnold *et al.* (2012), Santos *et al.* (2015), and Silva *et al.* (2018). This process was carried out automatically using the SWAT-CUP Sensitivity Analysis tool (SUFI-2) in the studied basin.

The 19 parameters considered for the sensitivity analysis were Alpha\_BF, Biomix, Canmx, CNII, CH\_K2, CH\_N2, Epc0, Esco, GW\_Delay, GW\_Revap, Gwqmn, Rchrg\_DP, Revapmn, Slsubbsn, Sol\_Al, Sol\_Awc, Sol\_K, Sol\_Z, and Surlag. The range of variation of each parameter and the change method that was used in the calibration process were defined based on the recommendations of Arnold *et al.* (2012) and de Medeiros *et al.* (2018). The results of the sensitivity analysis of the parameters were obtained after 500 iterations. The parameters considered most sensitive in the process of the sensitivity analysis were submitted to the automatic calibration process.

### Calibration, Validation, and Model Performance Evaluation

For the estimates of sediment yield in the Pirapama River basin, the SWAT model was previously calibrated and validated based on the comparison between the flow calculated by the model and the observed one. The calibration of the model was done in SWAT Calibration and Uncertainty Programs (SWAT-CUP) version 5.1.6.2.2012, developed by Abbaspour *et al.* (2007). SWAT-CUP integrates five semi-automatic calibration and uncertainty analysis procedures for the SWAT interface: SUFI2, PSO, GLUE, ParaSol, and MCMC. For this research, the Sequential Uncertainty Fitting algorithm (SUFI2) was used; according to Rouholahnejad *et al.* (2012), it uses the Latin hypercube method to define the parameters and the process starts with a range of values determined by the user.

Abbaspour *et al.* (2007) recommend that the number of iterations should be relatively large (500–1000); for this study, 500 iterations were done for each sub-basin analysed. Details about SWAT-CUP operation and calibration algorithms are described in Abbaspour (2012). According to Arnold *et al.* (2012), the first step of a calibration is to divide the observed values into two time series, one for calibration and one for validation. In the calibration, the input data are adjusted until a satisfactory result is obtained.

This phase considered the 12 parameters taken as more sensitive to flow adjustment for the study area, defined by the sensitivity analysis, by the literature, and by one of the SWAT developers (Dr Raghavan

Srinivasan). In addition, the same ranges and variation methods as were used in the sensitivity analysis were also considered, as shown in **Table 4**. After this procedure, the model was run for the validation period with the parameters adjusted in the calibration.

The performance of the model was verified through the objective functions: (4) Percent Bias (PBIAS), (5) the Nash-Sutcliffe coefficient (NS), and (6) the coefficient of determination ( $R^2$ ). PBIAS evaluates the average trend between simulated and observed data; NS looks for the best fit for the maximum flows and can range from infinite negative to 1, where 1 represents a perfect fit; and  $R^2$  measures the linear association between two variables, with the value obtained being dimensionless, ranging from 0 to 1, where the closer the value is to 1, the more efficient the prediction is. The ranges of values considered satisfactory were  $NS \geq 0.5$ ,  $PBIAS \leq \pm 25\%$ , and  $R^2 \geq 0.6$  (Moriassi *et al.*, 2007).

$$PBIAS = \frac{\sum_{i=1}^n (Q^{obs} - Q^{sim})}{\sum_{i=1}^n (Q^{obs})} \times 100 \quad (4)$$

$$NS = 1 - \left( \frac{\sum_i (Q_{obs} - Q_{sim})^2}{\sum_i (Q_{obs} - \overline{Q_{obs}})^2} \right) \quad (5)$$

$$R^2 = \left( \frac{\sum_{i=1}^n (Y_i - Y_m) \times (X_i - X_m)}{\sqrt{\sum_{i=1}^n (Y_i - Y_m)^2 \times \sum_{i=1}^n (X_i - X_m)^2}} \right)^2 \quad (6)$$

in which  $Q_{obs}$  is the measured flow rate,  $\overline{Q_{obs}}$  is the average observed flow,  $Q_{sim}$  is the simulated flow,  $n$  is the total number of observations,  $X_i$  are the observed values,  $X_m$  is the mean of these observed values,  $Y_i$  are the values calculated by the model, and  $Y_m$  is the average of these calculated values.

## Results and Discussion

### Flow calibration and validation

Based on the input data, the model was initially executed for flow simulation with no parameter changes. However, considering the need for adjustment, the calibration process was performed to improve the flow peaks and the base flow. In order to proceed with

**Table 4.** Parameters used for flow calibration for the study area

Parameter	Method	Range	
		Minimum	Maximum
ALPHA_BF	v	0	1
CANMX	v	0	10
CN2	r	-0.1	0.1
CH_K2	v	0	5
CH_N2	v	0	0.3
ESCO	v	0.5	1
GW_DELAY	a	-30	60
GW_REVAP	v	0.02	0.2
GWQMN	v	0	1000
REVAPMN	v	0	10
SOL_AWC	r	-0.25	0.25
RCHRG_DP	r	-0.04	0.05

**Table 5.** Parameters used in the calibration of the SWAT model, the methods used, and the fit values for each sub-basin.

Parameter	Methods	Calibrated values in stations	
		Cachoeira Tapada	Destilaria Inexport
ALPHA_BF	v	0.00243	0.17500
CANMX	v	5.77925	9.25000
CN2	r	-0.02273	-0.07500
CH_K2	v	5.74129	0.62500
CH_N2	v	0.24988	0.12750
ESCO	v	0.72832	0.76280
GW_DELAY	a	23.8410	53.2500
GW_REVAP	v	0.18932	0.18650
GWQMN	a	1012.41	675.000
REVAPMN	a	4.80460	0.75000
SOL_AWC	r	0.01305	-0.218805
RCHRG_DP	a	-0.01057	0.01175

Methods: v = replace (=), r = relative (x), and a = absolute (+).

the calibration, a sensitivity analysis was previously performed, where the 12 most sensitive parameters were adopted for the process of flow calibration for the Pirapama River basin. **Table 5** shows the parameters that were used in the calibration, the methods used, and the values adjusted after this process in the two contribution areas of the fluvimetric stations.

After the calibration phase, the peak flow and the base flow were adjusted in relation to the observed flow. **Figures 3a,b** and **4a,b** present the results of the correlation between the observed and simulated flows

by the SWAT model after the calibration and validation process for Cachoeira Tapada and Destilaria Inexport.

**Figure 3a** shows that the distribution of the data does not occur proportionally and that some of the data are overestimated by the model. However, most of the data are close to the 1:1 straight line, resulting in a good correlation with  $R^2 = 0.707$ . **Figure 3b** shows that in the validation period the data presented a good correlation, where it is possible to see values close to the 1:1 line and estimated values close to the observed ones, with  $R^2 = 0.852$ .

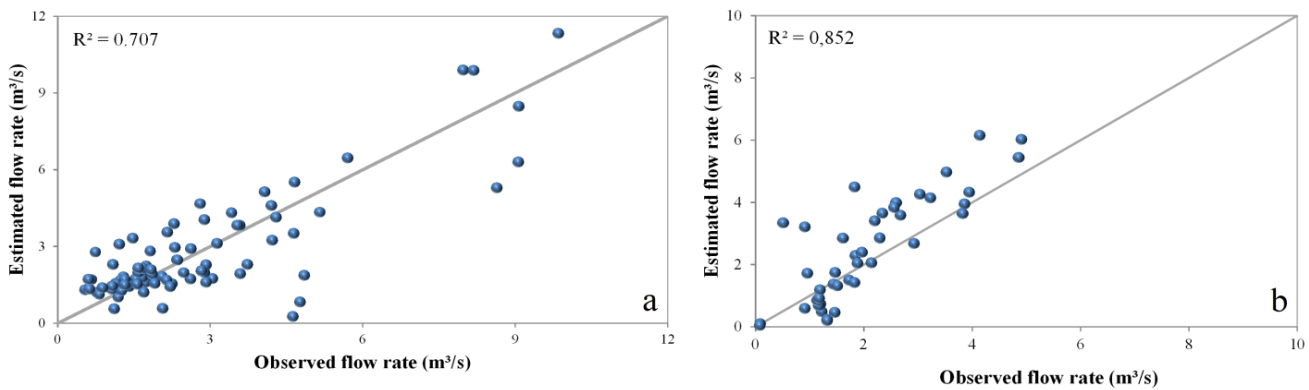


**Fig. 3** Correlation between the observed flow and that simulated by the model for Destilaria Inexport station for: (a) calibration (2000–2006), and (b) validation (2007–2010).

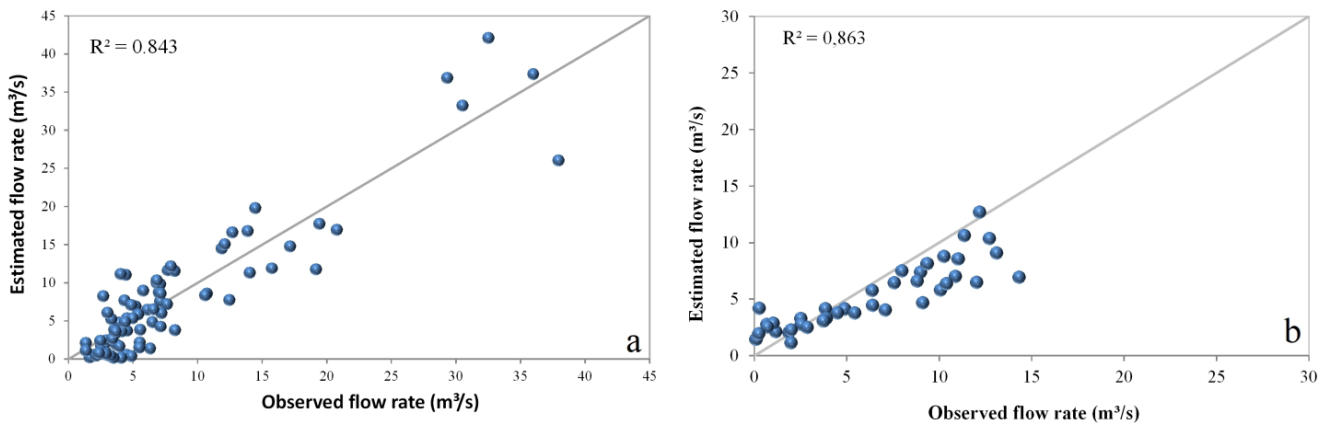


**Fig. 4** (a) Correlation between the observed flow and that simulated by the model for the fluvimetric station Destilaria Inexport (sub-basin 19), after the calibration (2000–2006) and (b) validation (2007–2010).

**Table 6.** Statistical data of the comparison between the observed flow and that simulated by the SWAT model after the calibration and validation process for the Cachoeira Tapada station.

Statistics	Calibration		Validation	
	Observed flow rate (m³/s)	Simulated flow rate (m³/s)	Observed flow rate (m³/s)	Simulated flow rate (m³/s)
Maximum	9.84	12.03	7.81	9.08
Minimum	0.54	0.27	0.08	0.05
Average	2.81	2.85	2.61	3.11
Standard deviation	2.21	2.31	1.85	2.31
R²	0.71		0.85	
NS	0.68		0.67	
PBIAS	1.46%		19.18%	



**Table 7.** Statistical data of the comparison between the observed flow and that simulated by the SWAT model after the calibration and validation for Destilaria Inexport streamflow station.

Statistics	Streamflow calibration		Streamflow validation	
	Observed (m <sup>3</sup> /s)	Simulated (m <sup>3</sup> /s)	Observed (m <sup>3</sup> /s)	Simulated (m <sup>3</sup> /s)
Maximum	37.94	42.10	24.00	24.95
Minimum	1.35	0.16	1.13	0.10
Average	7.92	7.74	7.38	8.79
Standard deviation	7.77	8.59	5.55	6.73
R <sup>2</sup>		0.84		0.86
NS		0.81		0.72
PBIAS		2.33%		-19.11%

From **Fig. 4a**, it can be seen that the distribution of the data does not occur proportionally, with a good part of the data between 0 and 10 m<sup>3</sup>/s being underestimated by the model. The larger flows have variability between the data, with simulated values being underestimated and overestimated. However, there is good correlation between the data, with R<sup>2</sup> of 0.84.

**Figure 4b** shows the result of the correlation between the simulated and observed flows after the validation process. It is possible to observe that in the validation period the data present a greater dispersion between the values when compared to the calibration period; however there is a good correlation among them, even with overestimated and underestimated values, with R<sup>2</sup> of 0.86.

**Table 6** presents the statistical data obtained in the calibration and validation of the model for the Cachoeira Tapada fluviometric station. It can be seen that in the calibration, the maximum simulated flow rate was overestimated by the model, with a difference of 2.19 m<sup>3</sup>/s. The minimum flow rate was underestimated by 0.27 m<sup>3</sup>/s and the average was almost equal to the observed value, with an overestimate of 0.04 m<sup>3</sup>/s. The standard deviation indicated that the simulated data varied more around the mean than the observed data, but the difference was very small (0.1 m<sup>3</sup>/s). Regarding the analysis of the performance of the model through the objective functions NS and PBIAS, the results of the calibration indicated that the simulated data are considered good for NS (0.68) and R<sup>2</sup> (0.71) and very good for PBIAS (1.46%), according to Moriasi *et al.* (2007).

Regarding the statistical data in the validation, **Table 6** shows that the maximum and average flow rates were overestimated by the model, with differences of 1.27 m<sup>3</sup>/s and 0.5 m<sup>3</sup>/s, respectively, from the observed values. The minimum flow rate was underestimated by 0.03 m<sup>3</sup>/s by the model in relation to the observed values. The standard deviation showed greater variation among the simulated values, with a difference of 0.46 m<sup>3</sup>/s from the observed one. The values of NS (0.67), R<sup>2</sup> (0.85), and PBIAS (19.18%) were considered good,

very good, and satisfactory, respectively (Moriasi *et al.*, 2007). In general, the statistical data showed that the results obtained in the calibration were better than those obtained in the validation, with the exception of R<sup>2</sup>.

**Table 7** presents the statistical data obtained in the calibration and validation of the model for the fluviometric station Destilaria Inexport. It can be seen that the maximum simulated flow rate was overestimated by the model, with a difference of 4.16m<sup>3</sup>/s. The minimum and average flow rates were underestimated, with differences of 1.19 and 0.18 m<sup>3</sup>/s, respectively. The standard deviation indicated that the simulated data varied more around the mean than the data observed after the calibration, with values of 7.77 m<sup>3</sup>/s (observed) and 8.59 m<sup>3</sup>/s (simulated). As regards the analysis of the performance of the model through the objective functions NS and PBIAS, the results of the calibration indicated that the simulated data are considered very good, according to Moriasi *et al.* (2007), with R<sup>2</sup> = 0.84, NS = 0.81, and PBIAS = 2.33% (**Table 7**).

In the validation, the simulated maximum flow rate was 0.95 m<sup>3</sup>/s higher than the observed one, the simulated minimum flow rate (1.03 m<sup>3</sup>/s) was higher than the observed one, and the simulated mean was higher than the observed mean, with a difference of 1.41 m<sup>3</sup>/s. The standard deviation showed a greater variation between the simulated values, with a difference of 1.18 m<sup>3</sup>/s from the observed one. The statistics showed values consistent with the literature, with NS = 0.72, R<sup>2</sup> = 0.86, and PBIAS = -19.11%. Therefore, the values of NS, R<sup>2</sup>, and PBIAS obtained after the validation can be considered good, very good, and satisfactory, respectively, according to Moriasi *et al.* (2007).

### Estimation of the sediment yield of the sub-basins of the Pirapama River Basin

After verifying that the model produced good results in the calibration and validation of the flow for the study area, it was applied to estimate the sediment yield by sub-basins for the period from 2000 to 2010. The

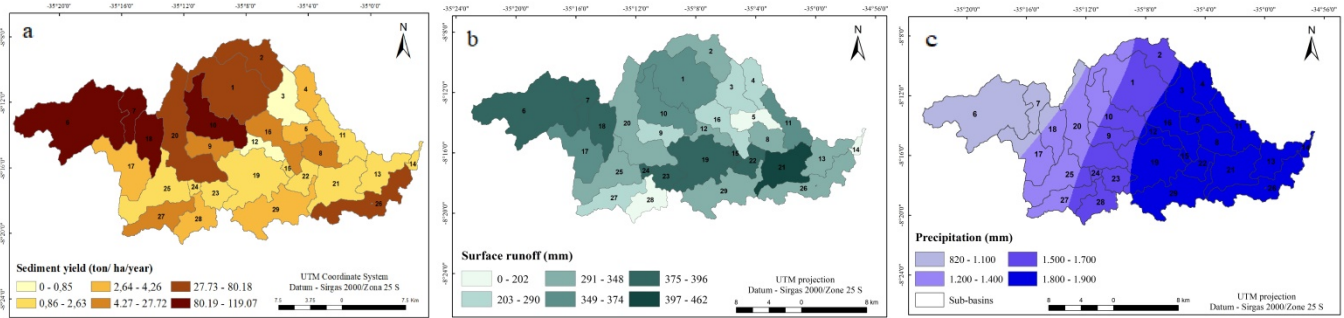


**Fig. 5** Spatial distribution of (a) sediment yield, (b) surface runoff, and (c) precipitation for Pirapama River basin between 2000 and 2010.

integration of the SWAT model and GIS was used to spatially analyse the distribution of sediment yield in the sub-basins, which was associated with the spatial distribution of surface runoff and precipitation, interpolated over the total area of the basin.

**Figure 5a** shows the spatial distribution of sediment production in the Pirapama River Basin for the period from 2000 to 2010. The estimate showed that the sediment yield of the sub-basins ranged from 0.85 to 119.07 ton/ha/yr. In the sub-basins where the fluviometric stations (17 and 19) are located, sediment yield ranged from 0.86 to 4.26 ton/ha/yr and surface runoff from 349 to 396 mm (**Fig. 5b**), with sub-basin 17 presenting the highest estimate of sediment yield among these sub-basins, with a value of 3.60 ton/ha.yr. With regard to precipitation, the highest values were found in sub-basin 19, whose area is closest to the coast, where precipitation varies between 1800 and 1900 mm (**Fig. 5c**).

In a general analysis, it was identified that the highest values of sediment yield are concentrated in the western and northern portions of the basin and the lowest in the eastern and southern portions (**Fig. 5a**). Some of the sub-basins that produced the highest amount of sediment (1, 2, 6, 7, 10, 18, and 20) also have high surface runoff values, varying between 291 and 396 mm (**Fig. 5b**). In these areas, precipitation varies from 820 to 1700 mm, unlike in the eastern portion of the basin, where there is a higher level of rain due to its proximity to the coast (**Fig. 5c**). Although these portions show a lower concentration of rainfall, they are more prone to erosion, as they are characterized by a predominance of sugarcane cultivation, pasture, and barren soil cover, which intensifies the erosion process. In addition, they have areas with sloping relief with predominance of Acrisols, which tend to be more susceptible to erosive processes, due to the texture relationship present in them, which leads to differences in infiltration of the surface and subsurface horizons.

A study by Silva and Santos (2008) in the Pirapama River Basin (1990 to 2001) found that the areas with the greatest slope contribute more to the erosion process when compared to flatter areas. The research showed

that erosion processes in the basin are influenced not only by rainfall in the region but also by slope, roughness, types of soil and land use. The authors further identified that the areas upstream of the Pirapama Reservoir (west of the basin) are potential locations causing silting of the dam.

Sub-basin 26 also had a higher sediment concentration, ranging from 27.73 to 80.18 ton/ha.yr, but is located in the eastern portion of the basin, whose area is more flate (**Fig. 5a**). In this region there are high levels of rainfall and diverse land use, characterized by agricultural areas, barren soil, pasture, dense vegetation, and urban areas, constituted by a small portion of the Cabo de Santo Agostinho city.

The surface runoff in this sub-basin ranged from 291 to 348 mm (**Fig. 5b**). The amount of rainfall and surface runoff, together with the different characteristics of the soil types (argisols, gleysol, nitisol, mangrove soils, and quartzarenic neosol) and soil uses, possibly favoured a larger sediment yield in this sub-basin relative to others of the same portion. In contrast, other sub-basins of the eastern and southern portions produced less sediment.

The Pirapama River basin is occupied by extensive areas of cultivation of sugarcane located in the basin. The cultivation of sugarcane is responsible for a higher sediment yield due to its management, considering that in the off-season of sugarcane, the soil is uncovered due to the harvest, contributing to greater soil particle disintegration, and transport of sediments by surface runoff (Aragão *et al.*, 2013).

Sub-basin 21 presented the highest runoff rate for the entire basin, varying between 397 and 462 mm, but produced less sediment than expected for the estimated quantity of runoff, which ranged from 0.86 to 2.63 ton/ha (**Figs. 5a, b**). This fact can be explained by the strong waterproofing of the soil present in the area of the sub-basin, due to the urban constructions and pavements found in the city of Cabo de Santo Agostinho, which occupies 32.90% of the sub-basin.

Sub-basins 3 and 12 had the lowest sediment yield among the sub-basins, varying between 0 and 0.85 ton/ha. The surface runoff varied between these areas,

ranging from 203 to 290 mm, 291 to 348 mm, and from 375 to 396 mm, respectively. Precipitation ranged from 1800 to 1900 mm. In general, although sub-basins 3 and 12 present characteristics that make them prone to higher sediment yields (rainfall and soil use), they are regions with a predominance of soils less prone to erosion (gleysol), with areas of dense vegetation on the slopes and smooth wavy and flattened relief. In this way, it is understood that the set of characteristics presented here led to a smaller production of sediments in the sub-basins of the Pirapama River.

The sediment yield obtained in this area of the basin is also similar to that found by Silva *et al.* (2015), who used SWAT in the San Francisco Subdivision watershed (area of 110,446.00 km<sup>2</sup>). The authors observed that the low risk areas predominate in the eastern and southeastern portions of the basin (near the outlet), due to the presence of relief associated with the flat meadow, with smooth wavy characteristics, which does not lead to large runoff and entrainment of the eroded material.

Santos *et al.* (2015) estimated the sediment yield in the Tapacurá River basin using the SWAT model. The authors verified that sediment yield in the region is directly related to surface runoff and precipitation as well as soil use and occupation characteristics. The study identified that in areas where agriculture predominated, sediment yield reached higher values, and in areas characterized by strong soil sealing by urban constructions, presented lower rates of sediment yield.

The research conducted by Makinde and Oyebanji (2018) in a Nigerian watershed using the Revised Universal Soil Loss Equation (RUSLE) showed that the sediment yield classified as very high and severe is located in regions with barren soil and cultivated land. The authors further concluded that the combination of rainfall and lack of cover for the topsoil produced high rates of soil loss in the study area.

Aga *et al.* (2018) made use of the SWAT model to predict the risk of erosion and sediment production in the Ziway River basin in Ethiopia. In this study, the authors found that some sub-basins with the same soil type, soil use, and steep slope produced a larger amount of sediment, indicating that the region's plateau is the main sediment transport source for the basin. With this, the authors emphasized that the variation of the sediment yield is more sensitive to the slope of the terrain in the region.

**Table 8** shows the means of precipitation, runoff, and sediment yield for the Pirapama River basin from 2000 to 2010. It can be observed that the largest sediment yield generated in the basin is related to the years with annual precipitation near or above the historical average of the period in the years 2003, 2009, and especially 2000. In the years in which the average annual precipitation was low in relation to the other years, as in 2001, 2006, and 2008, the average annual production of sediments was also lower than in the other years.

The study conducted by Silva and Santos (2008) using the Kinos hydrological model to model the Pirapama River basin from 1990 to 2001 showed that a large part of the basin is susceptible to the erosion process and that the year 2000 presented higher sediment yield for the studied area, being strongly related to the precipitation, whose average for the year was 3401 mm.

**Figure 6a** shows that sediment yield is strongly related to surface runoff, with the coefficient of determination showing a good correlation between these two variables (**Fig. 6b**), with R<sup>2</sup> of 0.91, close to the values found by Santos *et al.* (2015) in the Tapacurá River basin (0.98) and Silva and Santos (2008) in the Pirapama River basin (0.96), considering a period and hydrological model different from those used in this study.

**Table 8.** Means of precipitation, surface runoff, and sediment yield for the Pirapama River basin (2000–2010)

Year	Precipitation (mm)	Surface runoff (mm)	Sediment yield (ton/ha.yr)
2000	3408.80	996.82	171.55
2001	1463.30	168.93	33.08
2002	1793.90	300.15	71.41
2003	1854.90	330.57	86.03
2004	1754.40	322.20	73.40
2005	1851.50	301.81	52.92
2006	1652.80	211.20	49.09
2007	1901.50	294.01	57.52
2008	1569.40	218.25	52.85
2009	1967.80	343.08	78.47
2010	1595.50	260.02	57.87
Total average	1892.16	340.64	71.29

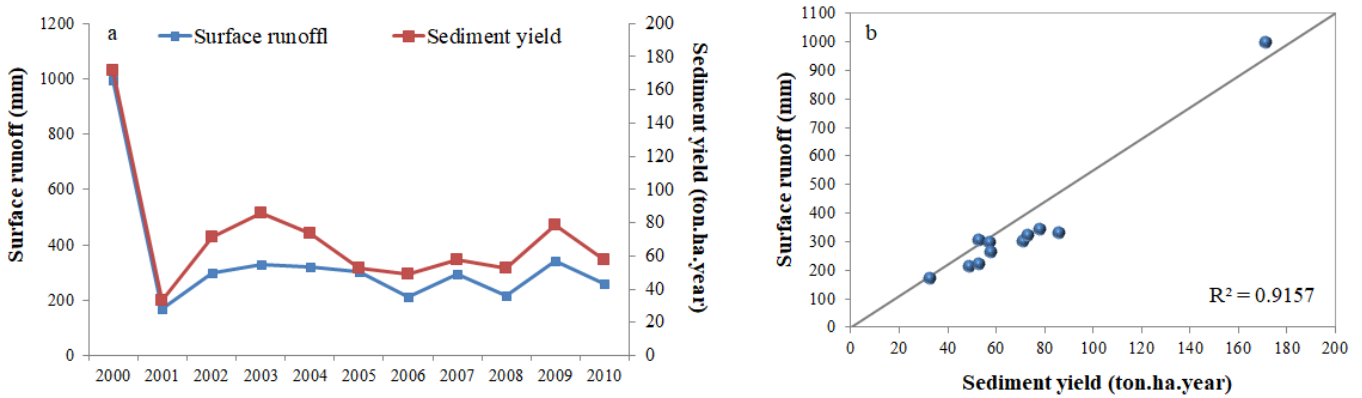


Fig. 6 (a) Relationship between the annual averages of surface runoff and (b) sediment yield in the Pirapama River basin from 2000 to 2010.

**Estimation of the total sediment supply for the Pirapama Reservoir**

Based on the sediment yield estimated by the SWAT model in the sub-basins of the Pirapama River basin, the annual sediment yield in the contribution area of the Pirapama Reservoir was estimated. According to the model classification, the contribution region of the reservoir drains an area of 341.94 km<sup>2</sup>, which represents 56.99% of the total area of the basin, and is found in 17 of the 29 sub-basins defined by the model (Fig. 7).

As can be observed in Fig. 7, the Pirapama Reservoir occupies part of the area of five sub-basins (12, 15, 16, 19, and 22) and its contribution network is located in the

portions of the basin that produced the most sediments, with soil losses of ranging from medium to strong, according to the classification proposed by Carvalho (2008).

Table 9 presents the mean precipitation, flow, and sediment yield of the Pirapama Reservoir contribution area between 2000 and 2010. According to the data presented in the table, the annual sediment yield for the area is directly related to precipitation as well as flow. The sediment yield presented higher values in the years 2000, 2002, 2003, 2004, and 2009, with estimates of 12.85, 6.03, 8.20, 6.34, and 7.07 ton/ha.yr, respectively. These years also presented high rates of

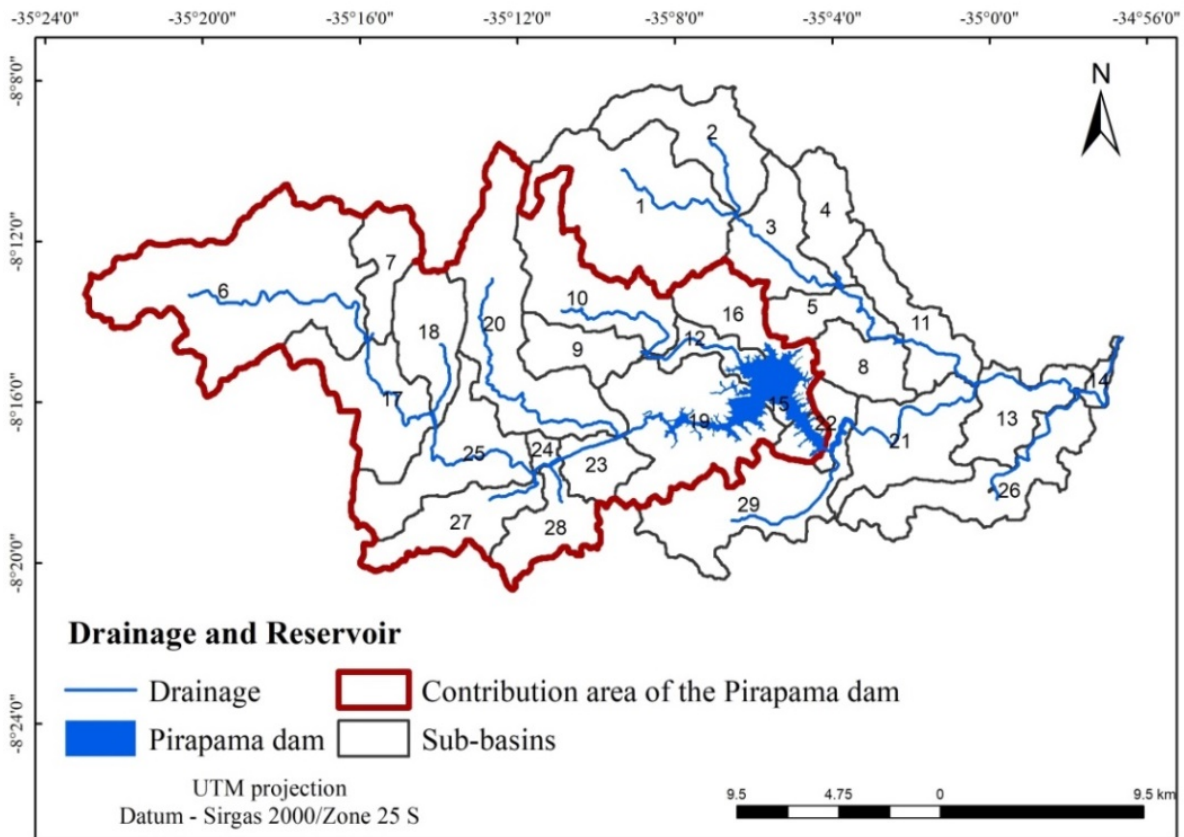


Fig. 7 Contribution area of the Pirapama Dam.

**Table 9.** Average precipitation, flow, and sediment yield of the area of contribution of the Pirapama Reservoir from 2000 to 2010.

Year	Precipitation (mm)	Flow rate (m <sup>3</sup> /s)	Sediment yield (ton/ha.yr)
2000	3408.80	8.76	12.85
2001	1463.30	2.74	1.88
2002	1793.90	3.75	6.03
2003	1854.90	3.94	8.20
2004	1754.40	4.08	6.34
2005	1851.50	4.08	3.12
2006	1652.80	3.10	3.15
2007	1901.50	4.43	3.98
2008	1569.40	3.37	3.90
2009	1967.80	4.48	7.07
2010	1595.50	3.02	4.32
Average	1892.16	4.16	5.53

precipitation and flow. The year 2001 had the lowest sediment yield (1.88 ton/ha.year), with lower precipitation and flow for the analysed period.

The mean sediment yield of the sub-basins of the Pirapama Reservoir contribution area was 60.84 ton/ha for the period analysed. According to the annual estimates performed, 5.53 ton/ha.yr of this amount are produced annually in this area, which corresponds to 9% of the soil losses over the period.

By estimating the fraction of sediment yield by each river stretch in the contribution area of the Pirapama reservoir (**Fig.8**), it was possible to list what was deposited and transported between the sub-basins of this area, especially in some of the areas where the Pirapama reservoir is located (15, 19 and 22). Through this relationship, it was estimated that about 3.12 ton of sediment was deposited in the Pirapama reservoir during the analyzed period.

In **Fig. 8** it is still possible to observe that in the river parts belonging to the sub-basins that receive no contribution from any other sub-basin (6, 7, 9, 10, 16, 18, 20, 27, 28), there is little or any deposition, ranging from 0.99 to 1.08 ton. On the other hand, as these areas show altimetric variation, the region positioned after the highest sub-basins is intersected by river parts where sediment deposition occurs. According to Santos et al. (2013), it can be stated that sediment deposition is mainly promoted by the sudden reduction of the slopes, since this configuration is capable of causing a decrease in river competence or capacity.

The river section that crosses the 6 (1 ton) and 7 (1 ton) sub-basins, for example, transport all sediment present in its segments to the next sub-basin 17 stream, whose slope is lower. Sub-basin 17 receives the sediment transported from these two sub-basins (6 and 7), equivalent to 2 tons, and carries only 31% of what it receives, ie 0.62 tons, retaining 1.38 tons in its area. According the estimated, deposition is now registred in sub-basin channels that have a smaller slope and are located in the main channel.

The rivers sections that presented the largest deposition were found in sub-basins 15, 17, 19 and 25, with values of 1.70, 1.38, 1.21 and 1.17 ton, respectively. Already the channels present in sub-basins 12, 23 and 24 carried practically everything they received for the following sections. For these sub-basins, sediment yield was lower, which is, mainly, explained by the less steep slope (**Fig.8**).

With regard to the average annual spatialization of the sediment yield generated for the contribution area of the Pirapama Reservoir, the results showed that, in general, the sub-basins located in the northern and western portions of the analysed area made higher contributions to the erosion process compared to some sub-basins of the southern and eastern portions (**Fig. 9**). According to this analysis, sediment yield was more significant in 2000, 2002, 2003, 2004, and 2009, with more than one sub-basin varying between 10 and 35 ton/ha.yr (**Figs. 9a, 9c, 9d, 9e, and 9j**). In addition to rain, the high sediment yield in these areas can also be explained by the fact that the steeper slopes are located in these areas (north and west), as discussed previously. In the annual analysis, the highest rates of sediment yield correspond to soil losses ranging from moderate to medium (Carvalho, 2008).

According to the results presented and discussed in **Table 9**, in the years with precipitation below the average of 1600 mm, the sediment production was lower than in the other years analysed, especially in the eastern and southern portions. The sub-basins of the eastern and southern portions produced less sediment in almost all the analysed years, with variation below 5 ton/ha.yr. According to Carvalho's classification (2008), the results for these sub-basins indicate null to small soil loss.

Thus, it was identified that the sub-basins upstream of the Pirapama Reservoir are portions of the basin susceptible to the erosion process, including sub-basin 19, where a good part of the reservoir is located (**Fig. 7**). These areas present physical and geomorphological characteristics prone to erosion. Sediment yield in

these portions can interfere with the volume of water of the Pirapama Reservoir, when the eroded material is carried to the depth of the lake. However, the estimates made by the model for this region could only be more reliable when compared with the observed sedimentological data. However, due to the lack of data on the local area, the estimates obtained by the model may represent an alternative way to monitor these areas more closely, since the flow was calibrated and validated, generating satisfactory results.

By way of comparison, Silva and Santos (2008) used the Kineros runoff-erosion model to quantify sediment production in the Pirapama River basin from 1990 to 2001. The study showed that the year 2000 presented a disparity in relation to the other years, as occurred in this study, with an average annual sediment value of around 276 ton/ha/ year and rainfall of 3,401 mm. However, Silva and Santos's study

reported sediment yield higher than that found in this study for the year 2000, which may be due to the differences between the models used and the information required by them.

Santos *et al.* (2015) applied the SWAT model to estimate and analyse the distribution of sediment yield in the Tapacurá River basin, State of Pernambuco, from 1995 to 2008. The study showed that the average sediment yield of the basin ranged from 0.10 to 22.99 ton/ha.yr, with an annual average of 7.67 ton/ha.yr. Santos *et al.* (2015) also pointed out, through data spatialization, that the highest values of sediment yield in the sub-basins were more concentrated in areas with a strong surface runoff, greater rainfall quantity, and a predominance of agriculture. The lowest rates of sediment yield were obtained in areas with strong soil sealing by urban constructions.

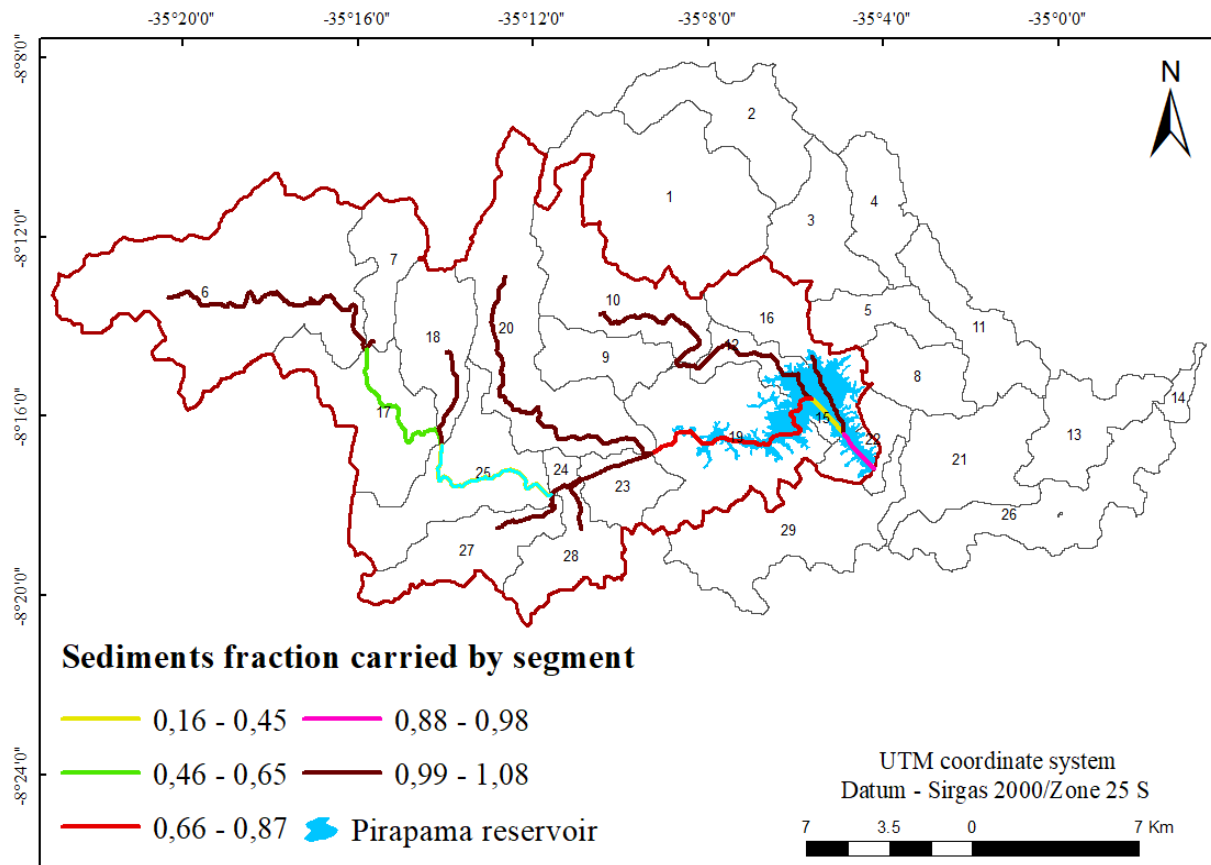
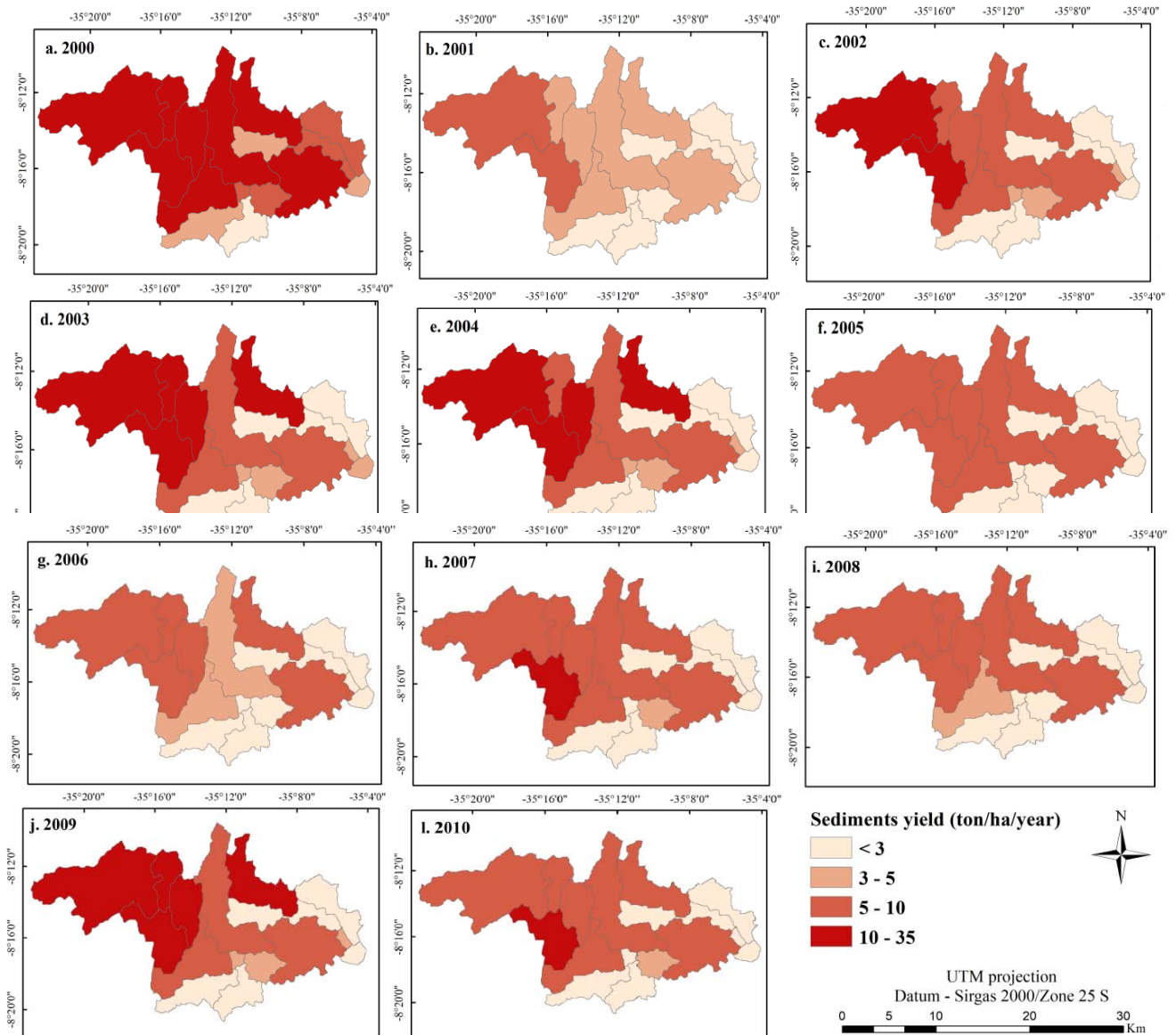


Fig. 8 Sediments fraction carried by segment in contribution area of the Pirapama Dam





**Fig. 9** Spatialization of estimated mean sediment yield for the contribution area of the Pirapama Reservoir between 2000 and 2010.

## CONCLUSIONS

Based on the results presented, it was observed that in the calibration of the model, using the flow variable, the estimated data had a good adjusted to the observed values, presenting results of NS,  $R^2$ , and PBIAS that ranged from very good to satisfactory in the two fluviometric stations analysed. The validation of the model also provided very good, good, and satisfactory results in the two fluviometric stations, with values higher than those considered acceptable by Moriasi *et al.* (2007).

The results of calibration and flow validation enabled coherent simulations of sediment yield when compared to surface runoff and precipitation. The spatialization of the results showed that the areas of the

basin that produce the highest amount of sediment are located in the northern and western portions. In these areas, the surface runoff was high, but the amount of rainfall in the region was lower than in other areas of the basin.

Although the level of precipitation in these portions has been lower than in other areas of the basin, the amount of rainfall is still high enough to influence the sediment yield rates of these areas. In addition, it was identified that these portions of the basin also have physical and morphological characteristics that intensify the erosion process. In contrast, most of the sub-basins of the southern and eastern portions produced less sediment, even though they had high rainfall and surface runoff in some of their sub-basins, which was explained by soil sealing in some sub-basins, plane

and/or smooth corrugated relief, and the presence of dense vegetation in some areas of slopes. Regarding estimates of annual sediment yield, it was verified that this variable is strongly related to precipitation and surface runoff, with higher sediment yields being identified at high rainfall and runoff levels. The results of annual flow and sediment yield estimates in the Pirapama Reservoir contribution area showed that these variables are directly related to precipitation. The annual spatialization of sediments yield by sub-basins in this region also indicated that the northern and western portions produce larger amounts of sediment annually, with moderate to medium soil loss, indicating that this region produced considerable sediment rates, according to high annual rates of precipitation and surface runoff, which may represent a risk of sedimentation and lower reservoir recharge capacity. However, the lack of measured sedimentometric data means that these estimates cannot be validated and qualified. Anyway, the estimates realized by the model may represent a way to monitor these sub-basins, since the flow was calibrated and validated with satisfactory results.

**ACKNOWLEDGMENTS** The authors thank the Foundation for the Support of Science and Technology of Pernambuco (FACEPE) for the doctoral scholarship of the first author and CAPES for the sandwich doctorate scholarship. They would also like to thank Texas A&M University, the SUPER project funded by CNPq (Proc. 446254/2015), the CNPq Universal Announcement Project (Proc. 448236/2014-1) for the PQ (Productivity and Research) grants of the second, third, fourth, and sixth authors, and the PEGASUS project MCTI/CNPq N° 19/2017 (Proc. 441305/2017-2).

## REFERENCES

- Abbaspour, K.C. (2012). SWAT-CUP 2012: SWAT Calibration and Uncertainty Programs – a user manual. Department of Systems Analysis, Integrated Assessment and Modelling (SIAM), Eawag, Swiss Federal Institute of Aquatic Science and Technology, Duessendorf, Switzerland, 103p.
- Abbaspour, K.C., Yang, J., Maximov, I., Siber, R., Bogner, K., Mieleitner, J., Zobrist, J., Srinivasan, R. (2007). Modelling hydrology and water quality in the pre-alpine/alpine Thur watershed using SWAT. *J. Hydrol.*, **333**, 413–430. [10.1016/j.jhydrol.2006.09.014](https://doi.org/10.1016/j.jhydrol.2006.09.014)
- Aga, A. O., Chane, B., Melesse, A. M. (2018). Soil Erosion Modelling and Risk Assessment in Data Scarce Rift Valley Lake Regions, Ethiopia. *Water* **10**, [10.3390/w10111684](https://doi.org/10.3390/w10111684)
- Aragão, R., Cruz, M.A.S., Amorim, J.R.A., Mendonça, L.C., Figueiredo, E.E., Srinivasan, V. S. (2013). Análise de sensibilidade dos parâmetros do modelo SWAT e simulação dos processos hidrossedimentológicos em uma bacia no agreste nordestino. *Rev. Bras. Ci. Solo*, **37**(4), 1091-1102.
- Arnold, J.G., Moriasi, D. N., Gassman, P. W., Abbaspour, K. C., White, M. J., Srinivasan R., santhi, C., Harmel, R. D., Van Griensven, A., Van Liew, M.W., Kannan, N., Jha, M. K. (2012). SWAT: model use, calibration, and validation. *Trans. ASABE*, **55**(4), 1491-1508.
- Arnold, J.G., Srinivasan, R., Mutiah, R.S. Williams, J.R. (1998). Large area hydrologic modeling and assessment part I: Model development. *J. Amer. Water Resour. Assoc.*, **34**(1), 1-17. [10.1111/j.1752-1688.1998.tb05961.x](https://doi.org/10.1111/j.1752-1688.1998.tb05961.x)
- Carvalho, N.O. (2008). Hidrossedimentologia prática. Rio de Janeiro: Editora Intercência.
- Corrado, S., Caldeira, C., Eriksson, M., Hanssen, O. J., Hauser, H.-E., van Holsteijn, F., Liu, G., Östergren, K., Parry, A., Secondi, L., Stenmarck, Å., Sala, S. (2019). Food waste accounting methodologies: Challenges, opportunities, and further advancements. *Global Food Security*, **20**, 93-100. [10.1016/j.gfs.2019.01.002](https://doi.org/10.1016/j.gfs.2019.01.002)
- CPRH – Companhia Pernambucana de Meio Ambiente (2003). Diagnóstico socioambiental do Litoral Sul de Pernambuco. Recife.
- de Medeiros, I.C., da Costa Silva, J.F.C.B., Silva, R.M., Santos, C.A.G. (2018). Run-off-erosion modelling and water balance in the Epitácio Pessoa Dam river basin, Paraíba State in Brazil. *Int. J. Environm. Sci. Technol.*, **15**, 1-14. [10.1007/s13762-018-1940-3](https://doi.org/10.1007/s13762-018-1940-3)
- den Biggelaar, C., Lal, R., Wiebe, K. (2003). The global impact of soil erosion on productivity II: effects on crop yields and production over time. *Adv. Agronomy* **81**, 49–95. [10.1016/S0065-2113\(03\)81002-7](https://doi.org/10.1016/S0065-2113(03)81002-7)
- EMBRAPA – Empresa Brasileira de Agropecuária (2013). Sistema Brasileiro de Classificação dos Solos. 3ª ed. Rio de Janeiro: EMBRAPA.
- Ghafari, H., Gorji, M., Arabkhedri, M., Ali Roshani, G., Heidari, A., Akhavan, S. (2017). Identification and prioritization of critical erosion areas based on onsite and offsite effects. *Catena*, **156**, 1-9. [10.1016/j.catena.2017.03.014](https://doi.org/10.1016/j.catena.2017.03.014)
- IBGE – Instituto Brasileiro de Geografia e Estatística (2007). Manual Técnico de Pedologia. Manuais Técnicos em Geociências. Ministério do Planejamento, Orçamento e Gestão. 2. edição. Rio de Janeiro: IBGE.
- IBGE – Instituto Brasileiro de Geografia e Estatística (2010). Censo Demográfico 2010. IBGE: Rio de Janeiro, 2010. Available in: [http://www.ibge.gov.br/home/estatistica/populacao/censo2010/sinopse/sinopse\\_tab\\_rm\\_zip.shtm](http://www.ibge.gov.br/home/estatistica/populacao/censo2010/sinopse/sinopse_tab_rm_zip.shtm), 2016. Accessed on 2018 October 27.
- Kirkby, M.J. (1990). Drainage basins and sediment transfer. In: *Geomorphology in environmental management* (Cooke, R. U. e Doornkamp, J. C. org.). 178-200. Oxford: Clarendon Press.
- Makinde, E.O., Oyebanji, E.I. (2018). The application of Remote Sensing and GIS Technology to erosion risk mapping. *Proceedings*, **2**, 1398. [10.3390/proceedings2211398](https://doi.org/10.3390/proceedings2211398)
- Medeiros Braga, A.C.F., Silva, R.M., Santos, C.A.G., Galvão, C.O., Nobre, P. (2013). Downscaling of a Global Climate Model for Estimation of Runoff, Sediment Yield and Dam Storage: A Case Study of Pirapama Basin, Brazil. *J. Hydrol.* **498**, 46–58. [10.1016/j.jhydrol.2013.06.007](https://doi.org/10.1016/j.jhydrol.2013.06.007)
- Moriasi, D.N., Arnold, J.G., Van Liew, M.W., Bingner, R.L., Harmel, R.D., Veith, T.L. (2007). Model evaluation guidelines for systematic quantification of accuracy in watershed simulations. *Trans. ASABE*, **50**(3), 885-900. [10.3390/10.13031/2013.23153](https://doi.org/10.3390/10.13031/2013.23153)
- Neitsch, S.L., Arnold, J.G., Kiniry, J.R., Williams, J.R. (2011). Soil and Water Assessment Tool – Theoretical Documentation Version 2009. Agricultural Research Service Blackland Research Center – Texas Agrilife Research. Texas A&M University System, 2011.
- Panagopoulos, Y., Makropoulos, C., Baltas, E., Mimikou, M. (2011). SWAT parameterization for the identification of critical diffuse pollution source areas under data limitations. *Ecological Model.*, **222**(19), 3500-3512. [10.1016/j.ecolmodel.2011.08.008](https://doi.org/10.1016/j.ecolmodel.2011.08.008)

- Pimentel, D., Harvey, C., Resosudarmo, P., Sinclair, K., Kurz, D., McNair, M., Crist, S., Shpritz, L., Fitton, L., Saffouri, R., Blair, R., 1995. Environmental and economic costs of soil erosion and conservation benefits. *Science* **267**, 1117–1123. [10.1016/j.ecolmodel.2011.08.008](https://doi.org/10.1016/j.ecolmodel.2011.08.008)
- Rouholahnejad, E., Abbaspour, K.C., Vejdani, M., Srinivasan, R., Schulin, R., Lehmann, A. A parallelization framework for calibration of hydrological models. *Environm. Model. Soft.*, **31**(1), 28-36, 2012. [10.1016/j.envsoft.2011.12.001](https://doi.org/10.1016/j.envsoft.2011.12.001)
- Santos, C.A.G., Silva, R.M. (2007). Aplicação do modelo hidrológico AÇUMOD baseado em SIG para a gestão de recursos hídricos do Rio Pirapama. *Ambi-água*, **2**(1), 1-14. [10.4136/ambi-agua.23](https://doi.org/10.4136/ambi-agua.23)
- Santos, J.Y.G., Silva, R.M., Carvalho Neto, J.G., Montenegro, S.M.G.L., Santos, C.A.G., Silva, A.M. (2015). Land cover and climate change effects on streamflow and sediment yield: a case study of Tapacurá River basin, Brazil. *Proc. Int. Assoc. Hydrol. Sci.*, **371**, 189-193. [10.5194/piahs-371-189-2015](https://doi.org/10.5194/piahs-371-189-2015)
- SECTMA – Secretaria de Ciência, Tecnologia e Meio Ambiente (1998). Plano Estadual de Recursos Hídricos do Estado de Pernambuco, v.1-3.
- Silva, R. M., Santos, C. A. G. Estimativa da produção de sedimentos mediante uso de um modelo hidrossedimentológico acoplado a um SIG. *Revista Brasileira de Engenharia Agrícola e Ambiental*, v.12, n.5, p. 520-526, 2008.
- Silva, R.M., Dantas, J.C., Beltrao, J.A., Santos, C.A.G. (2018). Hydrological simulation in a tropical humid basin in the Cerrado biome using the SWAT model. *Hydrol. Res.*, **49**, 908-923. [10.2166/nh.2018.222](https://doi.org/10.2166/nh.2018.222)
- Stretta, C. (2000). Hydrodynamic modelling of the Pirapama estuarine system after upstream regulation. Rapport INPT/ENSEEIH.